



*Citation for published version:*

Archila, HA, Brandon, D, Ansell, M, Walker, P & Ormondroyd, G 2015, 'Evaluation of the mechanical properties of cross laminated bamboo panels by digital image correlation and finite element modelling' Paper presented at World Conference on Timber Engineering (WCTE) 2014, Quebec City, Canada, 10/08/14 - 14/08/14, .

*Publication date:*  
2015

*Document Version*  
Peer reviewed version

[Link to publication](#)

## University of Bath

### General rights

Copyright and moral rights for the publications made accessible in the public portal are retained by the authors and/or other copyright owners and it is a condition of accessing publications that users recognise and abide by the legal requirements associated with these rights.

### Take down policy

If you believe that this document breaches copyright please contact us providing details, and we will remove access to the work immediately and investigate your claim.

# EVALUATION OF THE MECHANICAL PROPERTIES OF CROSS LAMINATED BAMBOO PANELS BY DIGITAL IMAGE CORRELATION AND FINITE ELEMENT MODELLING.

Hector F. Archila<sup>1</sup>, Daniel Brandon<sup>2</sup>, Martin P. Ansell<sup>3</sup>, Pete Walker<sup>4</sup>, Graham A. Ormondroyd<sup>5</sup>

**ABSTRACT:** *Guadua angustifolia Kunth* (Guadua) is a bamboo species native to South and Central America that has been widely used for structural applications in small and large scale buildings, bridges and temporary structures. Guadua remains a material for vernacular construction associated with high levels of manual labour and structural unpredictability. The aim of this work is to develop standardised industrial structural products from Guadua and to measure and predict their mechanical behaviour. Cross laminated Guadua (CLG) panels comprised of three and five layers were manufactured and their mechanical properties evaluated by testing large specimens in compression. The digital image correlation (DIC) method was applied to measure strain variations in the X, Y (in-plane) and Z (out of plane) axes on the surface of 600 mm<sup>2</sup> CLG panels. Strain results were analysed using VIC 3D software and used to calculate the elastic properties of the panels. Moduli of elasticity (MOE) values from DIC for three and five ply panels were 13.50 GPa and 22.59 GPa in the principal direction ( $E_0$ ) and 5.28 GPa and 12.54 GPa in the transverse direction ( $E_{90}$ ). Predicted MOE values for three and five ply panels were 20.76 GPa and 18.77 GPa in the principal direction ( $E_0$ ) and 10.80 GPa and 12.79 GPa in the transverse direction ( $E_{90}$ ). Results from predictions and DIC analysis were compared and a finite element (FE) model developed to predict the response of the CLG panels under similar load conditions. Overall, this study provides guidelines for structural design with engineered bamboo products which are of key importance for their mainstream use.

**KEYWORDS:** Bamboo, *Guadua angustifolia Kunth*, cross laminated panels, digital image correlation, compression test, in-plane diagonal shear test, finite element model.

## 1 INTRODUCTION

Bamboo-*Guadua angustifolia Kunth* (Guadua) has remarkable eco-credentials when compared to conventional building materials and exceptional advantages when compared to wood forest products. As with other bamboo species, Guadua is a fast growing non-wood forest resource that renews itself and has a high yield per hectare; it also captures and fixes more carbon than

most softwood trees [1], has an average density of about 800 kg/m<sup>3</sup> comparable to hardwoods of strength classes D30, D40 and D50 such as British Oak, Indian Teak and American White Oak, respectively [2].

Vogtländer *et al.* (2010), identified bamboo as one the best renewable resource in terms of yield when used in durable applications. Comparison of the annual yield of Guadua in m<sup>3</sup>/ha for products such as MDF is very similar to that of Eucalyptus and Radiata Pine [3] which makes Guadua a competitive alternative material for the production of panel products. Furthermore, bamboos in general have a considerable strength to weight ratio which is comparable to mild steel. Average values of elastic modulus per unit density (specific modulus) of bamboo are very similar to those of steel ( $25 \times 10^6 \text{ m}^2/\text{s}^2$ ) [4]. However, factors such as the bamboo species, its variation in density across and along the culm and anisotropic mechanical properties, as well as its rapid deterioration to when exposed to weather, hinder the use of bamboo in stiffness-driven applications where steel has been widely used. Engineered bamboo products are scarce and require complex manufacturing processes. For instance, fabrication of laminated Guadua

<sup>1</sup> Hector F. Archila-Santos, Department of Architecture and Civil Engineering, University of Bath, BA2 7AY, Bath, United Kingdom. Email: H.F.Archila.Santos@bath.ac.uk

<sup>2</sup> Daniel Brandon, Department of Architecture and Civil Engineering, University of Bath, BA2 7AY, Bath, United Kingdom. Email: D.Brandon@bath.ac.uk

<sup>3</sup> Martin P. Ansell, Department of Mechanical Engineering, University of Bath, BA2 7AY, Bath, United Kingdom. Email: M.P.Ansell@bath.ac.uk

<sup>4</sup> Pete Walker, Department of Architecture and Civil Engineering, University of Bath, BA2 7AY, Bath, United Kingdom. Email: P.Walker@bath.ac.uk

<sup>5</sup> Graham A. Ormondroyd, BioComposites Centre, Bangor University, Deiniol Road, Bangor, LL57 2UW, Gwynedd, United Kingdom. Email: g.ormondroyd@bangor.ac.uk

products results in an energy intensive process due to the machining of round culms into rectangular strips that produces high amounts of waste [3]–[5]. Therefore, the development of engineered Guadua products needs to exploit its remarkable features, tackle the issues regarding manufacture and improve issues regarding durability.

In order to tackle these challenges, thermo-hydro-mechanical (THM) treatments have been applied to Guadua with the aim of producing dimensionally stable densified flat Guadua sheets (FGS) with improved physical and mechanical properties. Studies on heat treatments applied to bamboo have shown improvements on the mechanical properties and resistance to termites and fungal decay [6], [7]. These studies and primary experimentation with THM modifications showed that temperatures below 160°C had a positive effect on the mechanical properties of Guadua and provided dimensionally stable flat Guadua sheets (FGS) with a densified profile [4]. These FGS were densified at the BioComposites Centre, Bangor University, then arranged in a cross laminated fashion, glued using a high performance epoxy resin and cold-pressed to manufacture cross laminated Guadua (CLG) panels. Following a period of curing, the panels were subjected to a testing programme with the aim of characterising their mechanical properties and a finite element model (FEM) was developed. Digital image correlation (DIC) techniques were used to track the physical deformation and strain in the panels under load. This paper reports on the development of CLG panels at the University of Bath and presents the results from mechanical testing, DIC analysis and FEM simulation. Overall, the CLG panels were manufactured using straightforward densification and assembly methods that could be easily applied industrially.

## 2 MANUFACTURE OF CLG PANELS.

### 2.1 PREPARATION OF THE MATERIAL

Round culms of Guadua were cut to the required length and their outermost layers were removed using a professional burnisher fitted with a 100 mm x 289 mm x 40 grit Zirconium cloth belt. This highly abrasive belt was used to remove about 100µm of the tough cutinized layer that covers the cortex of Guadua. Subsequently the peeled lengths of cylindrical Guadua were radially cut into six to eight strips (depending on the diameter) and the inner pith cavity membrane was also removed.

The strips were stored under controlled temperature (27°C ± 2°C) and relative humidity (70 ± 5%) in a conditioning room, enabling them to reach equilibrium at 12% moisture content (MC). By following the above mentioned process a reduction of 27% in wasted material was achieved [4].

### 2.2 DENSIFICATION

Following immersion in water for 24 hours, the strips were subjected to an open THM treatment for 20 minutes using

a daylight opening hot press with 1000 square mm oil heated platens. Pressure on the hydraulic press was computer controlled using PressMAN software and applied across the radial direction. Maximum pressure, temperature and compression set were fixed at 50 kg/cm<sup>2</sup>, 150°C and 45% respectively (Figure 1b). The compression set (C) is defined as  $C = (Ro - Rc) / Ro$  where Ro and Rc are the thickness of the samples before and after compression respectively.

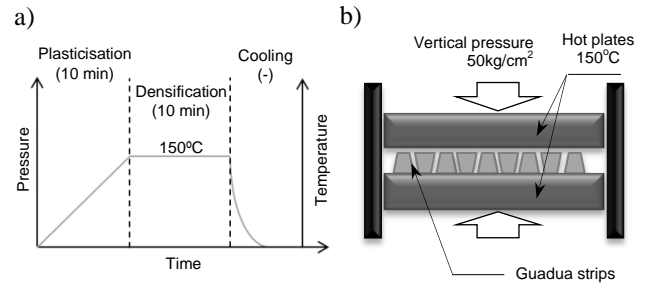


**Figure 1.** (a) THM diagram. (b) Diagram of the heat and pressure process.

As can be seen in Figure 1a, THM modification occurred in two stages; the first is a plasticisation stage where temperature and pressure on the strips of Guadua is increased for 10 minutes. The second is the densification stage, where maximum pressure and temperature were maintained for 10 minutes. This densification process provided densified FGS with improved mechanical properties. Elastic values for the FGS were obtained by longitudinal tensile testing and compression testing tangential to the direction of the Guadua fibres. Some of these results have been previously reported by the author [4] and are summarized on Table 1. A slight reduction in the dry weight of the strips was recorded post-THM treatment; however, the MC was not significantly affected (reduced by -0.5%).

**Table 1.** Characteristic elastic values and Poisson's ratio of FGS pre and post THM modification.

Property	Pre-THM (raw Guadua)	Post-THM (FGS)
$E_{L(Tension)}$	16.88 ± 4.22 GPa	30.72 ± 3.51 GPa
$E_{T(Compression)}$	0.55 ± 0.23 GPa	0.84 ± 0.01 GPa
$V_{LT}$	0.28 ± 0.02	0.26 ± 0.04
$V_{LR}$	0.30 ± 0.01	0.079 ± 0.18
Compression set (C)	0 %	42.51 %
Density (ρ)	540 kg/m <sup>3</sup>	830 kg/m <sup>3</sup>
Specific stiffness (average)	31.25 m <sup>2</sup> s <sup>-2</sup>	37.01 m <sup>2</sup> s <sup>-2</sup>

### 2.3 LAMINATION

FGS were arranged in consecutive layers at  $0^\circ$  and  $90^\circ$  angles to form the individual plies of three and five layer (CLG-3 & CLG-5) cross laminated Guadua panels. These plies were glued with a mix of wood epoxy resin (Sicomin SR 5550) and wood gap filler (Wood fill 250), which also increased the viscosity of the mix. The content of resin by total weight of the composite was 4% and the spreading rate was  $215 \text{ g/m}^2$ . Cold pressure of about  $35 \text{ kg/cm}^2$  was applied to the panels until the resin was set and then left to cure in a conditioning room at controlled temperature ( $27^\circ\text{C} \pm 2^\circ\text{C}$ ) and relative humidity ( $70 \pm 5 \%$ ) for about 20 days before machining. Figure 2 illustrates the different stages of the lamination process and details of the resulting panels.

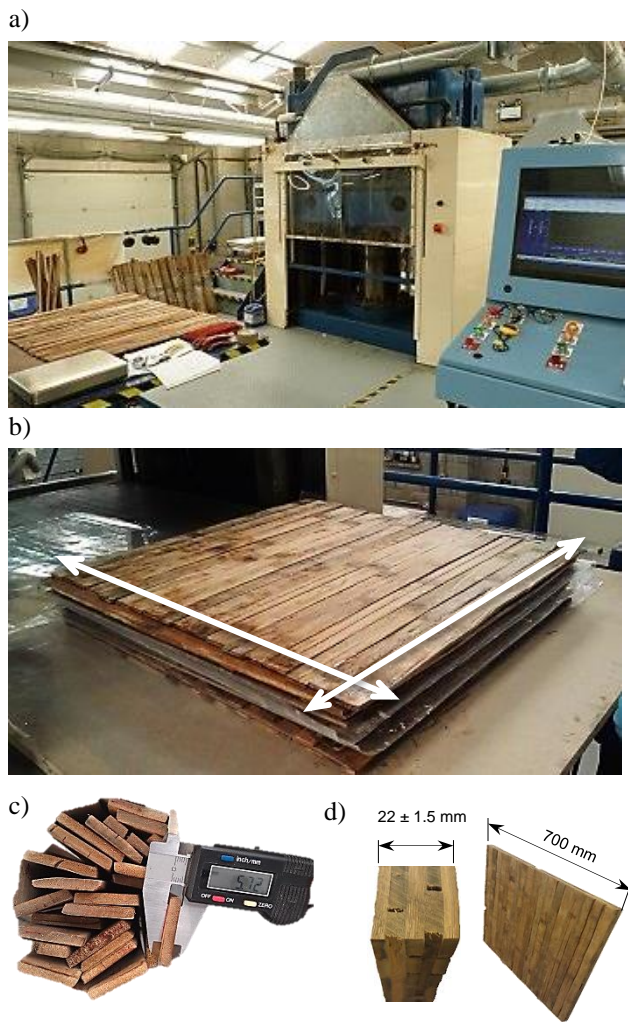


**Figure 2.** a) Daylight opening hot press used for densification of Guadua strips and cold pressing of panels. b) Cross lamination of FGS to form CLG panels of three and five layers. c) Guadua strips after densification (FGS). d) Average thickness and size of the CLG manufactured for testing.

The laminate panel comprised an odd number of layers (three and five) with alternating layers with a regular

thicknesses of  $5.5 \pm 0.3 \text{ mm}$  disposed at  $0^\circ$  and  $90^\circ$ . For structural analysis the CLG-3 and CLG-5 panels are considered as shell elements under plane stress conditions that require the evaluation of their orthotropic elastic properties (MOE, shear modulus and Poisson's ratio).

The longitudinal orientation of the CLG panels corresponds to its load bearing direction and is defined by the orientation of Guadua fibres in the outer layers (Figure 3a). This also represents the highest number of layers orientated in  $X_1$  with a ratio of 2 to 3 for CLG-3 and 3 to 5 for CLG-5.

## 3 EXPERIMENTS AND ANALYSIS

### 3.1 COMPRESSION TESTS

CLG-3 and CLG-5 panels of  $600 \text{ mm} \times 600 \text{ mm}$  were tested in compression in the  $X_1$  (longitudinal) and  $X_2$  (transverse) directions as illustrated in Figure 3. The panels were tested according to the BS EN 789:2004 [8] standard for structural timber elements. Compression tests of the panels were carried out in a 200 kN Mayes universal test machine (Figure 4) at a rate of  $0.5 \text{ mm/min}$ . Ten loading series below the elastic limit were undertaken per panel and special test fixtures were used to anchor the panels to the test machine.

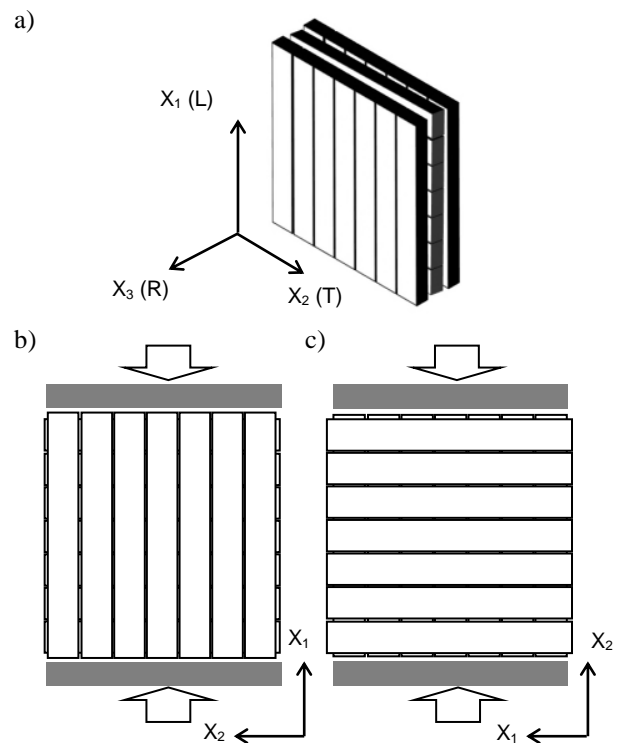
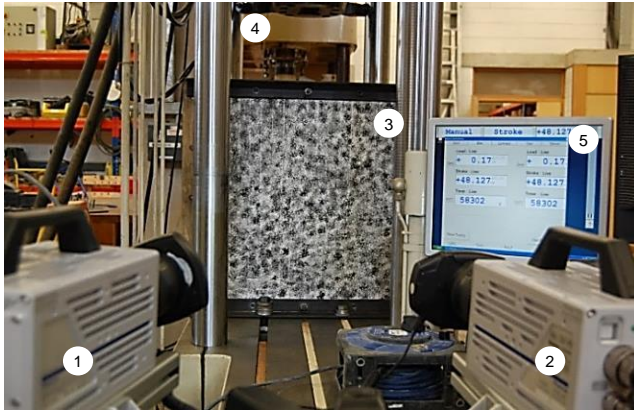


**Figure 3.** a) Geometric ( $X_1$ ,  $X_2$ ,  $X_3$ ) and orthotropic (L, R, T) axis of a CLG-3 panel. b) Diagram of the compression test in the longitudinal direction of the panel. c) Diagram of the compression test in the transverse direction of the panel.

### 3.2 DIGITAL IMAGE CORRELATION METHOD

During mechanical testing, two monochrome high speed cameras (Fast Cam SA3) recorded simultaneous images of a speckle pattern painted on the surface of the panel at a rate of one frame per second (Figure 4). Both cameras were positioned at a stereo angle below  $60^\circ$  and care was taken to achieve sharp focus, adequate illumination and correct brightness. Prior to test, a calibration grid that covered the full field of view was positioned in front of the panel and a set of approximately 60 images were recorded. These images were then analysed using the calibration tool of the VIC3D-2009 software and a low overall error was ensured before running the test.



1 & 2. High speed cameras; 3. CLG panel; 4. Test machine; 5. Monitor

**Figure 4.** Typical setup for the compression test of CLG panels using the DIC method.

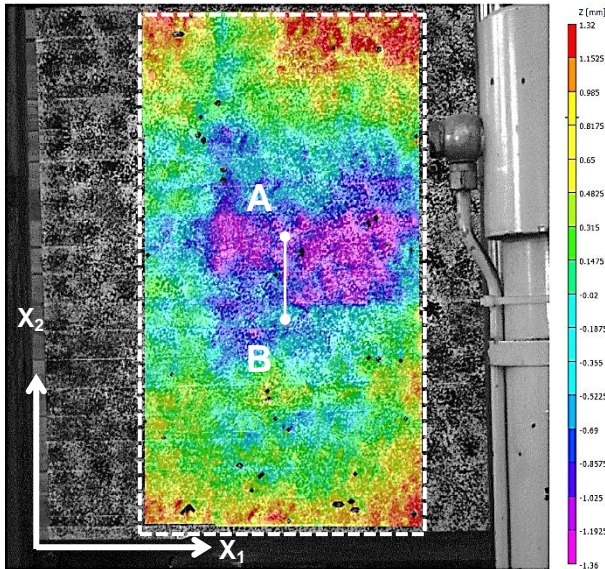


**Figure 5.** Strain map in  $X_3$  (radial) direction of a CLG panel tested in compression along  $X_2$  (transversal) axis.

During test, the cameras captured the increase in load from a monitor (Item 5 in Figure 4) placed to one side and the corresponding deformations in the X, Y (in-plane) and Z

(out of plane) axes of the panel. It was then possible to track both load and strain for each pair of images at a rate of one image per second. These sets of paired images were analysed using VIC3D-2009 software and 3D strain maps were produced (Figure 5 & 6).

A virtual extensometer (A-B) was placed on the face of the panel within the speckle pattern and the axial strain variations per image were recorded. Figures 5 and 6 illustrate the area analysed and the location of the extensometer.

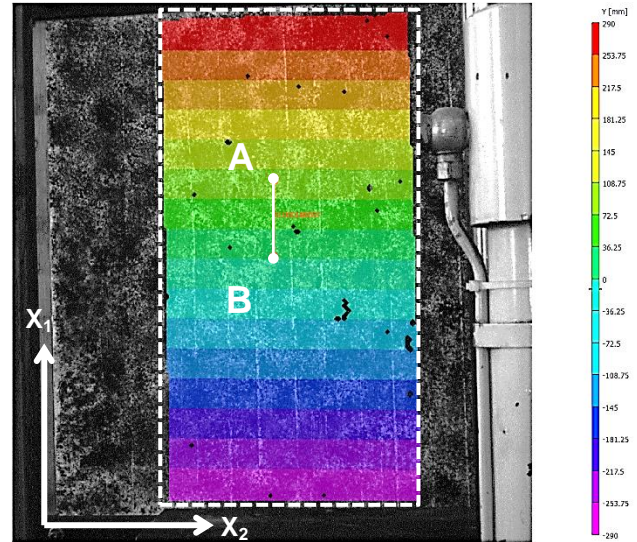


**Figure 6.** Strain map resulting in  $X_1$  of a CLG panel tested in compression along  $X_1$  (longitudinal) axis.

### 3.3 FINITE ELEMENT MODEL (FEM)

FEMs of the three and five layers CLG panels were developed using ABAQUS/CAE 6.10-2 to simulate the elastic behaviour of the panels under similar load conditions to the compression tests previously undertaken. For the analytical predictions of the compression stiffness it was assumed that plane cross sections remain plane and, therefore, no shear stress between the  $0^\circ$  and  $90^\circ$  elements of the panel occurred. This, however, is not realistic as there were gaps present between parallel lamellae of the manufactured CLG panels. Hence, orthogonal behaviour was assumed for the model and elastic properties presented in Table 1 and a rolling shear value of 0.581 MPa reported by [9] were used for the analysis.

Finite element analyses were undertaken to study the influence of the gaps. FEMs were developed for 3-layered and 5-layered panels (CLG-3 and CLG-5) and loaded in both in-plane directions ( $X_1$  and  $X_2$ ). For the FEMs, the total height and width of the panel is 600 mm and all configurations were modelled with and without gaps. The widths of the individual strips (FGS) modelled are 30 mm for the models with gaps and 33 mm for the gapless

models, respectively. The thickness of each layer is 5.5 mm and the width of the gaps is 3 mm.

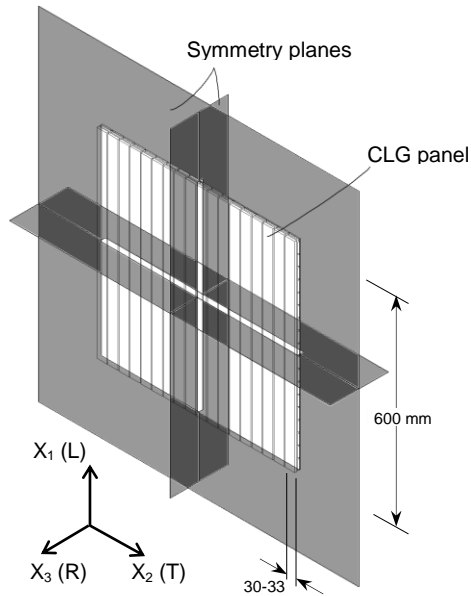


**Figure 7.** Symmetry planes of the tested CLG panel.

It can be observed in Figure 7 that the panel has three symmetry planes, thus only 1/8 of the actual panel is modelled. The parts that are not modelled can be simulated by boundary conditions. To replicate a symmetry plane, all out of plane translations and rotations have to be restrained. Geometry of the 1/8 model can be seen in Figure 8. Grey surfaces indicate the boundary conditions, whilst black surfaces on the top of the panel indicate that load is only applied to the lamellae with the grain direction parallel to the load (L).

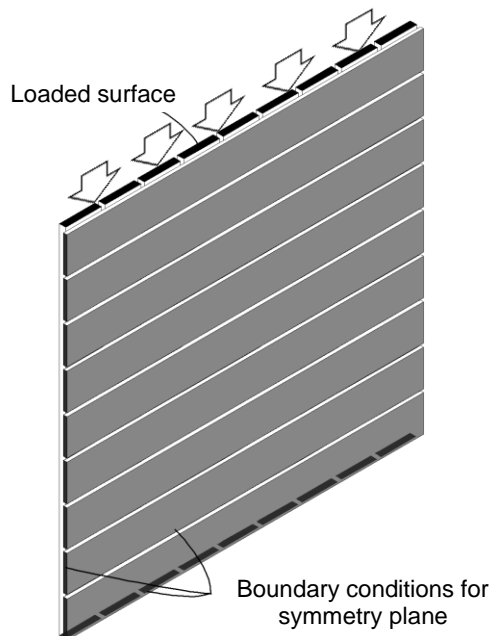


**Figure 8.** Location of boundary conditions in FEM.

The elements used for the analysis were 3 dimensional linear 8-node elements with reduced integration. Each element has only one integration point which is located in the centre of the element. This element type is prone to *hourglassing*, which occurs when the element is bent. The strain in the centre of the element is then zero which leads to zero energy modes and an overestimation of deflections. The *enhanced hourglass control* function of ABAQUS was applied to avoid this *hourglassing*. The mesh was composed of four elements in the thickness direction of the lamellae ( $X_3$ ) to be able to simulate shear deformations. In the other two directions the element size was kept at 3 mm which is equal to the gap size. By doing this, the nodes of the lamellae that were in contact coincided. Normal *hard contact* described the behaviour of two lamellae parallel to each other. In this contact a *master* and *slave surface* are chosen, where the slave nodes cannot penetrate the master surface. Since the mesh and material properties of both lamellae were similar, the master and slave surfaces could be randomly chosen. The glued connection between two crossing lamellae was simulated with *tie constraints*. The nearest nodes of both members were tied together and could not move relatively to each other. As the surface nodes of contacting members coincided in the model, the coinciding nodes behaved as one.

### 3.4 DETERMINATION OF MOE

Strain values from the DIC method were used to calculate the MOE of CLG-3 and CLG-5 panels in the longitudinal ( $E_0$ ) and transverse direction ( $E_{90}$ ). Typical stress-strain response obtained from the compression test of three and five layers CLG panels was plotted and a linear regression analysis was performed (Figure 9).

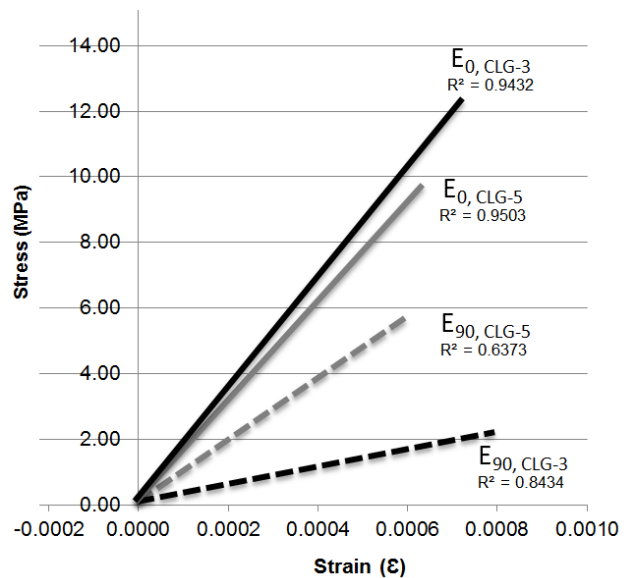


**Figure 9.** Typical strain-stress graph for CLG-3 and CLG-5 panels tested in the longitudinal direction (0) and transverse (90) direction.

Values for stress and strain obtained from the longest linear portion of the graph between  $0.1F_{\max}$  and  $0.4F_{\max}$  with a correlation coefficient  $\geq 0.60$  were input into Equation (1) to determine the compression moduli of elasticity (MOE),  $E_0$  and  $E_{90}$ .

$$E_c = \frac{(F_2 - F_1)l}{(u_2 - u_1)A} \quad (1)$$

where

$F_2 - F_1$  is the increment of load between  $0.1F_{\max}$  and  $0.4F_{\max}$

$u_2, u_1$  is the increment of load corresponding to  $F_2 - F_1$

$l$  is the length of the gauge length (A-B length of the virtual extensometer), and

$A$  is the cross sectional area of the panel.

For the analytical prediction of the average MOE in compression in the parallel ( $E_0$ ) and transverse ( $E_{90}$ ) directions of the panel, calculation methods for the derivation of the mechanical properties of plywood were used [10]. This method is in accordance with Equation (2) and Table 2 presents the typical procedure followed for the determination of the panel modulus in compression ( $V_{pc}$ ) with loading direction  $E_0$ .

$$V_{pc} = \frac{U_p}{T} = \sum_{i=1}^{i=n} t_i \times V_{i,c,t} / \sum_{i=1}^{i=n} t_i \quad (2)$$

where

$U_p$  is the panel stiffness,

$t_i$  is the thickness of the individual layer, and

$V_i$  is the characteristic MOE of the individual layer.

**Table 2** Calculation of a CLG-5 panel modulus in compression ( $V_{pc}$ ) for the longitudinal direction summed from layers 1 to 5.

Layer no.	Layer direction	$t_i$ (mm)	$k_{ai}$	$V_i$ (GPa)	$U_{pi} = t_i \cdot k_{ai} \cdot V_i$ (kN/mm)
1	0°	5.5	1	30.72	168.96
2	90°	5.5	1	0.84	4.62
3	0°	5.5	1	30.72	168.96
4	90°	5.5	1	0.84	4.62
5	0°	5.5	1	30.72	168.96

$$V_{pc} = \frac{U_p}{T} \quad T = \sum_{i=1}^{i=n} t_i = 27.5 \text{ mm} \quad U_p = \sum_{i=1}^{i=n} U_{pi} = 519.12 \frac{\text{kN}}{\text{mm}}$$

$$V_{pc} = E_{0,CLG-5} = 18.77 \text{ GPa}$$

The MOE of the panels ( $V_{pc}$ ) can be defined as the ratio of the summation of the individual stiffnesses of each layer – depending on their orientation 0° or 90°- ( $U_{pi}$ ) to the summation of the thicknesses of the individual layers ( $T$ ) where  $V_{i,0}=E_L=30.72$  GPa and  $V_{i,90}=E_T=0.84$ GPa.  $k_{ai}$  is a modification factor related to the surface appearance of the face layers and is assumed to be one. The rest of the predicted values for the different configurations of the

CLG panels are presented in Table 3. This table also contains the results for MOE in compression for both directions ( $E_0$  and  $E_{90}$ ) of CLG-3 and CLG-5 panels using the DIC-method and the finite elements (FE) analysis.

**Table 3.** Modulus of elasticity in compression longitudinal ( $E_0$ ) and transverse ( $E_{90}$ ) directions of the CLG panels determined analytically, by the DIC method and FE analysis.

MOE Values	$E_{0,CLG-3}$	$E_{90,CLG-3}$	$E_{0,CLG-5}$	$E_{90,CLG-5}$
DIC-Test	13.50 GPa	5.28 GPa	22.59 GPa	12.54 GPa
Predicted	20.76 GPa	10.80 GPa	18.77 GPa	12.79 GPa
FEM (gapless)	20.69 GPa	10.75 GPa	18.70 GPa	12.66 GPa
FEM (with gaps)	18.75 GPa	9.56 GPa	16.94 GPa	11.42 GPa

No significant variation is observed between the calculated results and the values obtained through the FE analysis. This validates the accuracy of the FEM. Predicted MOE values were generally higher than the MOE values obtained through the DIC method. CLG-3 and CLG-5 panels longitudinally oriented presented a load capacity between 1.5 and 2.5 times their transverse orientation in both predicted and test results. No permanent deformation (post-test) in either axis of the load application ( $X_1$  and  $X_2$ ) was recorded by the DIC; however, 3D strain maps showed areas prone to deformation in the  $X_3$  (R) direction in the CLG-3 panel (Figure 10-11). This particular panel possessed localized gaps due to fabrication defects. Hence, the fairly low test result obtained for  $E_{90,CLG-3}$  can be explained by the presence of gaps in the panel. Results from the FEM for the CLG panels with gaps also demonstrated the influence that gaps can have on the overall compressive stiffness of the CLG panels which was reduced by about 10%.

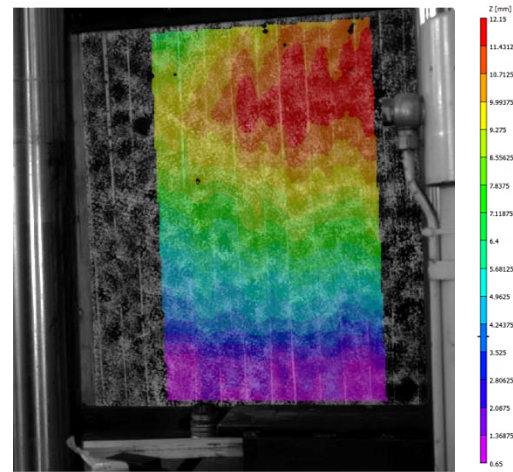


**Figure 10.** Front view of the 3D strain map of the deformation in  $z$  ( $X_3$ ) of the CLG-3 panel tested in compression  $E_0$ .

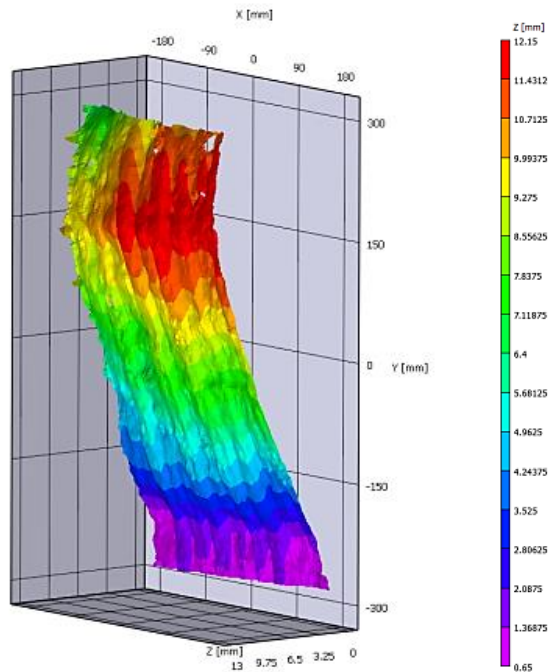


**Figure 11.** Axonometric view of the 3D strain map of the deformation in  $z$  ( $X_3$ ) of the CLG-3 panel tested in compression  $E_0$ .

## 4 CONCLUSIONS

The viability and benefits of applying THM treatments for the manufacture of engineered bamboo products were proven by the research project. Flat cross-laminated *Guadua* (CLG) panels were manufactured using a simplified process that reduced the wastage produced during conventional lamination processing by 27% [4] and improved mechanical properties.

Mechanical properties of the CLG panels were calculated using characteristic elastic values obtained from previous tests of small clear specimens, characterised through mechanical testing using the digital image correlation (DIC) method and validated with a finite element model (FEM). Results obtained proved the load bearing capacity of the panel and improved mechanical properties when compared to elastic values for engineered timber products. Average values for MOE in compression of CLT-3 and CLT-5 panels with larger cross sectional areas than the CLG panels are: 7.42 GPa and 6.74 GPa in the longitudinal direction ( $E_0$ ) and 4.62 GPa and 3.91 GPa in the transverse direction, respectively. Fairly similar MOE values in longitudinal compression ( $E_{0,5ply} = 14$  GPa) have been reported [11] for cross laminated bamboo products using different manufacturing and testing techniques. This highlights the potential of bamboo engineered products as substitutes for wood in engineering applications.

Validation of the results will require further testing using physical strain measurement systems. DIC methods produced a qualitative assessment of the structural

behaviour of the panels, but difficulties were encountered in the quantitative analysis of their mechanical properties.

## ACKNOWLEDGEMENT

The first author is grateful to AMPHIBIA GROUP LTD and COLCIENCIAS, sponsors of his studies at the University of Bath, UK.

## REFERENCES

- [1] Y. Lou, Y. Li, K. Buckingham, H. Giles, and G. Zhou, "Bamboo and Climate Change Mitigation Bamboo: a comparative analysis of carbon sequestration. INBAR Technical Report No. 32," Beijing, People's Republic of China, 2010.
- [2] J. Marcroft, "Concise Eurocodes: Design of Timber Structures. BS EN 1995-1-1: Eurocode 5," London, UK, 2012.
- [3] J. Vogtländer, P. van der Lugt, and H. Brezet, "The sustainability of bamboo products for local and Western European applications. LCAs and land-use," *J. Clean. Prod.*, vol. 18, no. 13, pp. 1260–1269, Sep. 2010.
- [4] H. F. Archila-Santos, M. P. Ansell, and P. Walker, "Elastic Properties of Thermo-Hydro-Mechanically Modified Bamboo (*Guadua angustifolia* Kunth) Measured in Tension," in *Key Engineering Materials*, 2014, vol. 600, pp. 111–120.
- [5] K. Flander and R. Rovers, "One laminated bamboo-frame house per hectare per year," *Constr. Build. Mater.*, vol. 23, no. 1, pp. 210–218, Jan. 2009.
- [6] Y. M. Zhang, Y. L. Yu, and W. J. Yu, "Effect of thermal treatment on the physical and mechanical properties of *phyllostachys pubescens* bamboo," *Eur. J. Wood Wood Prod.*, vol. 71, no. 1, pp. 61–67, Nov. 2012.
- [7] R. D. Manalo and C. M. Garcia, "Termite Resistance of Thermally-Modified *Dendrocalamus asper* (Schultes f.) Backer ex Heyne," *Insects*, vol. 3, no. 4, pp. 390–395, Mar. 2012.
- [8] BSI, "BS EN 789:2004, Timber structures — Test methods — Determination of mechanical properties of wood based panels," 2004.
- [9] J. J. García, C. Rangel, and K. Ghavami, "Experiments with rings to determine the



anisotropic elastic constants of bamboo,” *Constr. Build. Mater.*, vol. 31, pp. 52–57, 2012.

- [10] BSI, “BS EN 14272:2011, Plywood — Calculation method for some mechanical properties,” London, UK, 2011.
- [11] C. S. Verma and V. M. Chariar, “Development of layered laminate bamboo composite and their mechanical properties,” *Compos. Part B Eng.*, vol. 43, no. 3, pp. 1063–1069, Apr. 2012.